Energy and Buildings 75 (2014) 531–537

Contents lists available at ScienceDirect

Energy and Buildings

journal homepage: www.elsevier.com/locate/enbuild

Thermal analysis of a new solar kang system

Ming Yang[a,*], Xudong Yang[b], Zhifeng Wang[a], Pengsu Wang[b]

[a] Key Laboratory of Solar Thermal Energy and Photovoltaic System, Institute of Electrical Engineering, Chinese Academy of Sciences, Beijing 100190, PR China
[b] Department of Building Science, Tsinghua University, Beijing 100084, PR China

ARTICLE INFO

Article history:
Received 3 May 2013
Received in revised form 19 February 2014
Accepted 23 February 2014

Keyword:
Developing country
Solar energy storage
Residential heating
Solar air heaters

ABSTRACT

The solar kang, which integrates the positive features of the solar air collecting system and the conventional Chinese kang, could serve as a low-polluting heating device alterative to the traditional kang, feasible for the rural households in northern China. On the basis of the dynamic heat transfer model developed in the previous work, we conducted a series of numerical parametric analysis in the light of energy storage of the kang body, energy distribution, and temperature variations of the upper kang plate. It was found that the solar kang body normally absorbed most of the airflow heat input due to large convective heat transfer area in the air space. The thermal physical parameters of the upper kang plate, including the thermal capacity and the thermal conductivity, had significant influence on the kang's heat transfer process and the according temperature variations. The results from this numerical study could be useful for the thermal design of such new local heating systems.

1. Introduction

At present, around 100 million tons of coal is consumed every year for heating in northern rural China, which results an emission of around 300 million tons of CO_2, 1 million tons of SO_2, and 70 million tons of NO_x [1]. Development of new feasible technologies for housing heating is considered as a critical way to decrease solid fuel use and improve indoor/outdoor air quality in developing countries.

The Chinese kang, serving as a heated bed that normally recovers thermal energy from a solid fuel cooking stove, is widely used as a local heating device in northern rural China [2]. However, the cook stove usually emits high level of pollutants due to low combustion efficiency of solid fuels, usually straw, wood and other biomass residues, resulting significant health challenges [3]. To tackle this problem, we have developed a new Chinese solar kang system, which integrates the low-cost, easily maintained solar air collecting system and the traditional kang system, as Fig. 1 presents, to reduce certain amount of non-clean energy use [4]. In the solar kang system, solar energy is firstly stored in the kang body by the convective heat transfer with the warm airflow, which is circulated from the solar air heater into the hollow cavity of the kang body by a small fan during the daytime. The heat is released into the room gradually when the kang body gets sufficiently warm. The traditional solid fuel stove, fume space and chimney are still accommodated in the new system, serving as the auxiliary heating system with consideration of uncertain weather conditions and cost effectiveness.

To better understand the thermal performance of this new house heating system, in this study, we began by introducing the dynamic heat transfer model briefly, and then singled out three parameters based on the thermal model and the heat transfer process. A series of numerical parametric analysis on the new kang body in consideration of energy storage of the kang body, energy distribution and temperature variations of the upper kang plate was then carried out on the basis of model simulation. Experiments were conducted to validate the simulation results under certain circumstances.

2. The dynamic heat transfer model and validation

2.1. The model

The model of the integrated system has three parts according to the thermal process, including the model of the heating source (the solar air heater and the stove), the kang body, and the room. The model of the solar air heater could be developed either by the detailed heat transfer process (white box model) [5] or the collector efficiency equation (black box model) [6], and an equivalent heat

* Corresponding author. Tel.: +86 1013810622739; fax: +86 1062587946.
E-mail addresses: yangming717@vip.qq.com, yangming07@gmail.com (M. Yang).

http://dx.doi.org/10.1016/j.enbuild.2014.02.047
0378-7788/

Nomenclature

A	heat transfer matrix
B	thermal disturbance matrix
C	thermal capacity matrix
C_p	specific heat (J/(kg K))
F	heat transfer area (m^2)
h	heat transfer coefficient (W/(m^2 K))
s	heat storage coefficient (24 h) (W/(m^2 K))
T	temperature matrix
Ratio	the interior surface area of the upper kang plate/the exterior surface area of the upper kang plate, the interior surface area equals the convection heat transfer area between the airflow and the upper kang plate.
Q	heat (MJ)
V	volume (m^3)

Subscripts

ka	airflow in the kang air space
ka,kp	from the airflow to the kang plates
ka,kpi	from the airflow to the kang plate *i*
*ka,k*1	from the airflow to the upper kang plate
*ka,k*2	from the airflow to the south kang plate
*ka,k*4	from the airflow to the north kang plate
*ka,k*5	from the airflow to the west kang plate
*ka,k*6	from the airflow to the east kang plate
kf	fume in the kang fume space
kpi	kang plate *i*
room, *k*1	from the room to the upper kang plate
*kp,k*1	from the other kang plates to the upper kang plate
*e,k*1	internal energy of the kang plate
par	partition plate

Greek letters

$\tau_{charging}$	thermal charging period
λ	thermal conductivity (W/(m K))
ρ	density (kg/m^3)

power could be employed to replace the complicated burning process simulation in the stove model [2]. The dynamic heat transfer model of the room was developed based on the state space method used in a building energy simulation program DeST [7,8], which considers the dynamic heat conduction in the envelop, internal surface long-wave radiation, convection with indoor and outdoor air, and multi-zone interaction by conduction and ventilation.

The heat transfer process of the solar kang is so different from the conventional kang, and the model of the solar kang is thus the innovative point of the integrated system and developed under the following assumptions that:

1. Both the air and fume are considered as an ideal gas.
2. The gas flow is fully mixed either in the air or the fume space.
3. The airflow inside the kang air space has a uniform velocity.
4. Temperatures of the kang plates only vary along the thickness.
5. There is no leakage between the air and fume space.
6. The effect of wind is ignored, meaning that smoke always flows upward from the stove to the chimney during the firing time, and the fume mass flow is only driven by the buoyancy force in the fume system.

Based on the coupled heat transfer process between the air, fume, and the thermal storage of the kang plates, the dynamic

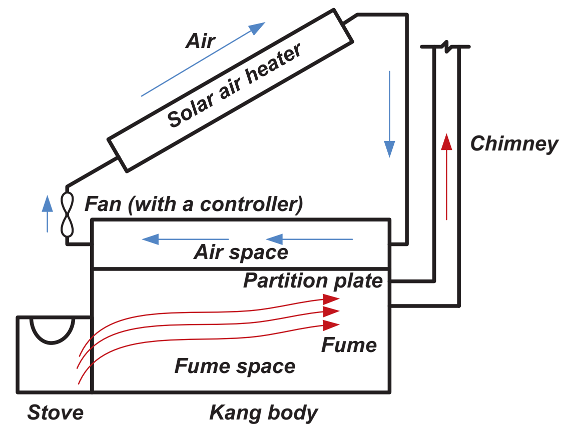

Fig. 1. Schematic view of the solar kang system with supplemental heat from the stove.

thermal process of the kang body could be finally transformed into the matrix form as Eq. (1):

$$C\dot{T} = AT + B \tag{1}$$

where, the diagonal matrix C is the thermal capacity matrix of the kang body, having close relationship with the thermal capacity $C_p\rho V$ of each kang plate. B is called the thermal disturbance matrix, mainly influenced by the solar irradiance on the kang plate and the other heating resources in the room. The symmetric matrix A is the heat transfer matrix, which is closely related to the convective heat transfer resistance in the air space, view factors between different kang plates, thermal conductivity of the kang plate, and the comprehensive heat transfer resistance between the kang and the room. T is the temperature matrix, also the solution of Eq. (1).

An iterative procedure is employed to simulate the kang system. The component temperatures of the kang body could be calculated after assuming the indoor air temperature, and finally adjusted until all the temperature differences between the guessed and calculated values are less than 0.1 °C. It is noticed that the solar air heater normally would not work with positive efficiency when there is solid fuel burning due to the high inlet air temperature of the heater. Therefore, there are three typical working scenarios in the whole day: only fan (solar air heater) is on, only firing (stove) is on, and there is not any heating source to heat up the kang body. Each working scenario could be realized by setting the working schedule of the fan and stove in the model. For more details about the model of solar kang system please refer to the detailed model of the solar kang system [4].

2.2. Model validation

An experiment, to validate the accuracy of the theoretical kang body model, was carried out in the Rural Energy and Environment Laboratory of Tsinghua University, located in the suburb of Beijing, China. The test space contains two test rooms and one auxiliary room. The layout of the test room and the solar kang system is presented in Fig. 2, and detailed physical information on each component is shown in Table 1. A conventional solar air heater, with solar collecting dimensions 2 m (length) × 2 m (width), was located at the south window of the test room 2 to provide solar heat during the daytime. A conventional stove, which is used for providing heat during the night by burning wood, was located in the auxiliary room.

The test was carried out from January 17 to January 20, 2011, which was almost the coldest period in Beijing. The outdoor air temperature varied from −15 to 10 °C, and the maximal solar irradiance

Table 1
Physical properties of the test room and the kang system.

	Component	Thickness (mm)	ρ (kg/m^3)	λ (W/(m K))	C_p (J/(kg K))	S (W/(m^2 K))
Test room						
External wall	Solid brick wall	370	1800	0.81	880	9.65
	EPS	50	30	0.04	1380	0.36
	Cement	20	1800	0.93	840	10.10
Interior wall	Solid brick wall	120	1800	0.81	880	9.65
	Cement	20	1800	0.93	840	10.10
Roof	Waterproof	20	600	0.17	1470	3.33
	Precast concrete slab	150	1600	0.81	840	8.90
	Cement	20	1800	0.93	840	10.10
Floor	Concrete	150	2500	1.74	920	17.20
	Cement	20	1800	0.93	840	10.10
Window	Double plastic-steel window	Heat transfer coefficient is 3.0 W(m^2 K)				
Kang body						
Upper/bottom plate	Precast concrete slab	50	1600	0.81	840	8.90
	Cement	10	1800	0.93	840	10.10
Vertical plate	Solid brick	60	1668	0.43	750	6.26
	Cement	10	1800	0.93	840	10.10
Partition plate	Iron	4	7753	52.00	490	–
Chimney						
Chimney	Iron	1	7753	52.00	490	–

on the solar collecting area changed between 800 and 1000 W/m^2. The fan was set to work when the outlet air temperature of the solar air heater was higher than the interior surface temperature of the upper kang plate, normally from 9:30 to 15:00 during the test. The wood burning was set to last from 16:00 to 17:30, and the inlet of the kang fume space was sealed after burning, ensuring that there was no or little airflow once the firing process was completed.

Temperatures at the kang plates, as well as in the kang air space and fume space were measured, and results were compared with the simulation results. Considering the asymmetric temperature distribution of the kang and the interior surfaces of the envelop, several temperature measuring points were put uniformly on these surfaces and along the fume flow direction to get the average values. Besides that, all the measured temperatures were checked by the heat flux of each kang plate on the basis of the energy conservation, ensuring that the measurement data were reliable.

The measured and simulated temperature variations of the air and fume temperatures in the kang body, as well as the upper kang plate are shown in Figs. 3 and 4, respectively. It is shown that the main trend of the simulation and measurement was in accordance although there were some discrepancies, which were possibly caused by testing point positions, leakage between the air and fume space, and computational error of the empirical formulas used in the model. Nevertheless, the dynamic heat transfer model of the solar kang could present the thermal performance of the new kang body, and is used for the following thermal analysis.

3. Parametric analysis

The heat transfer process of the solar kang is very different from the conventional kang, and thus the parametric analysis on the new kang body is considered as the key point in this paper. According to the normal evaluation standard, the kang body, serving as some thermal storage equipment, is normally regarded to work with better thermal performance if it could absorb more convection heat transfer under the same airflow heat input the kang body during the thermal charging period, and release heat into the room during the desired period, such as night.

Based on the heat transfer process, the energy stored in the kang body, also the convection heat transfer from the warm airflow to the interior surfaces of the kang plates $Q_{ka,kp}$, could be expressed as:

$$Q_{ka,kp} = \int_{\tau_{\text{charging}}} \sum_i h_{ka,kpi} F_{kpi} (t_{ka} - t_{kpi}) \cdot d\tau \qquad (2)$$

It is presented from the above equation that $Q_{ka,kp}$ is mainly determined by the convective heat transfer resistance in the kang air space, normally defined as $1/(hF)$ [9]. The less the convective heat transfer resistance is, the more the airflow heat would transfer to the kang plates, and that may eventually lead to the higher energy storage under the same airflow heat input. In order to present the thermal performance of the kang body, the thermal performance of either the solar air heater or the stove is not included in the following parametric analyses.

In the heat transfer process between the kang body and the room, many factors have impact on the heat release of the kang body, such as the thermal construction of the kang and the room, view factors between different kang plates, comprehensive heat transfer coefficients between the kang and the room, etc. In this paper, we chose to consider the thermal impact of the thermal capacity $C_p \rho V$ and the thermal conductivity λ of the upper kang plate, in terms of presenting the thermal storage performance of the solar kang itself.

Next, serial numerical analyses of the above three parameters were conducted by changing one parameter at a time on the basis of the "base case" scenario. Their impacts on the kang body's thermal performance were compared under the same working condition in the light of energy storage of the kang body, energy distribution and the temperature variations of the upper kang plate.

3.1. Base case study

The test room and the solar kang system mentioned above, shown in Fig. 2 and Table 1, were used as the calculation conditions in the base case. The weather condition in the simulation is shown in Fig. 5. With consideration of the thermal mass of the kang and room, the first 26 days of simulation was for eliminating the impact of the initial guessed values [8], and there was no heat input the kang body during this period to ensure that the kang with different parameters could work with the same initial thermal state in the last two days, and make the results comparable. Moreover, only solar air heater worked for heating the kang in the last two days in the simulation, and thermal wave input the kang body is

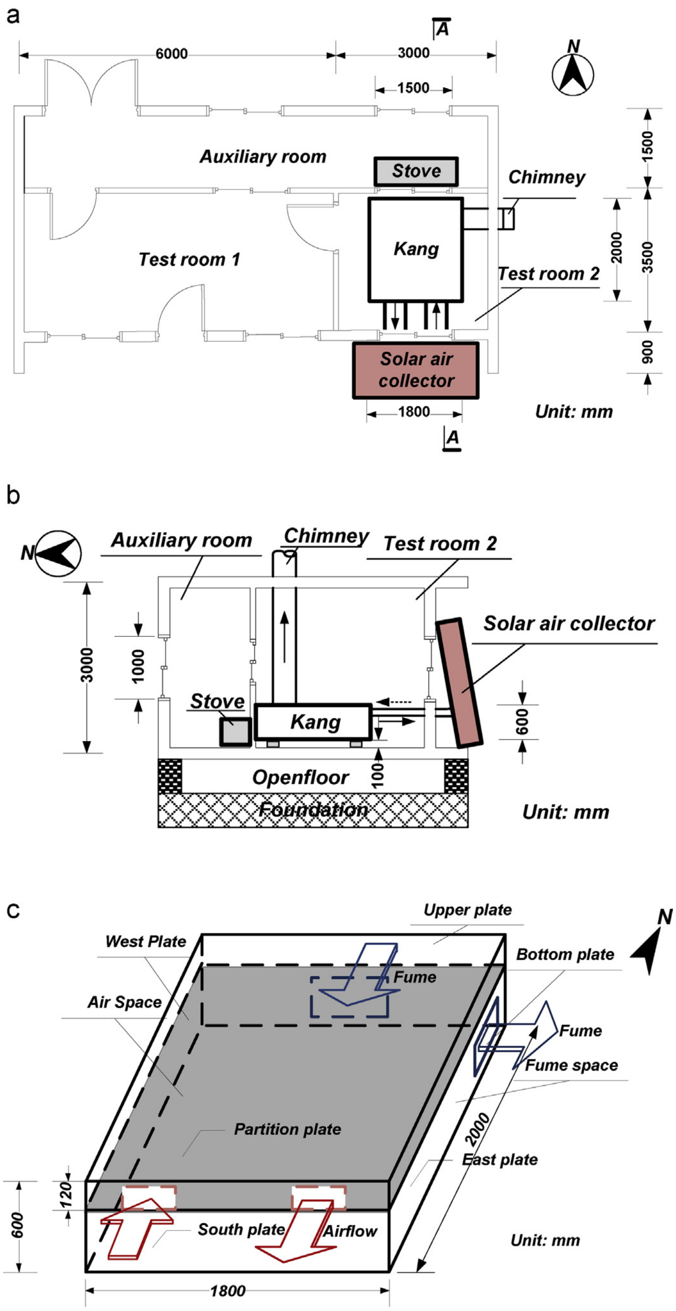

Fig. 2. Layout of the test room and the kang system, (a) ichnographic view, (b) profile view (A-A), (c) the solar kang body.

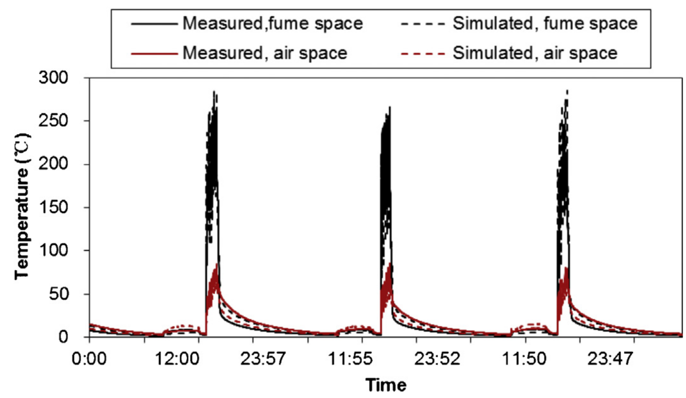

Fig. 3. Measured and simulated temperatures of the fume and air space in the kang body.

presented in Fig. 6, with total airflow volume rate 500 m^3/h. During the whole simulation period, there was not any other heating source in the room and the solar irradiance from the south window was obstructed by an opaque object, such as black-out cloth, ensuring that there was no thermal disturbance on the kang body.

Fig. 7 presents the periodical temperature variations of the upper kang plate, changing with the thermal wave input the kang body. The maximal temperature of the interior surface of the upper kang plate could be as high as around 30 °C, while that of the exterior surface around 25 °C. Meanwhile, the time delay of these two surfaces was about 2.5–3.0 h due to the kang's thermal mass. It is also shown in Fig. 7 that the temperature of the upper kang plate at the end of the simulation period was higher than the initial state, meaning that part of the heat input turned into the internal energy of the kang, and this is visually expressed in accumulated energy distribution of the kang body, as Fig. 8 presents. Additionally, Fig. 8 also presents that 78% of the total airflow heat input was transferred to the kang body by convection between the warm airflow and the walls of the kang air space under the calculation condition during the thermal charging period. Then, this amount of heat transformed into the heat release into the room (around 67% of the total airflow heat input) and the internal energy of the kang body (about 11% of the total airflow heat input) gradually during the calculation period. It is also noticed that the upper kang plate releases the most part of the heat, around 42% during the simulation period, while the other kang plate releases around 3% –7% of the total heat input, respectively. Based on such heat transfer process, it could be observed that:

- The solar kang body could serve as a high-efficient thermal storage terminal, which could absorb most of the airflow heat during the charging period.
- The most proportion of the solar heat could be stored in the upper kang plate compared with the other plates due to large convective heat transfer area between the upper kang plate and the airflow.

3.2. The impact of the convective heat transfer resistance in the kang air space

Decreasing the convective heat transfer resistance is beneficial to strengthen the convection heat transfer, and thus may help to increase energy storage of the kang body, and eventually be

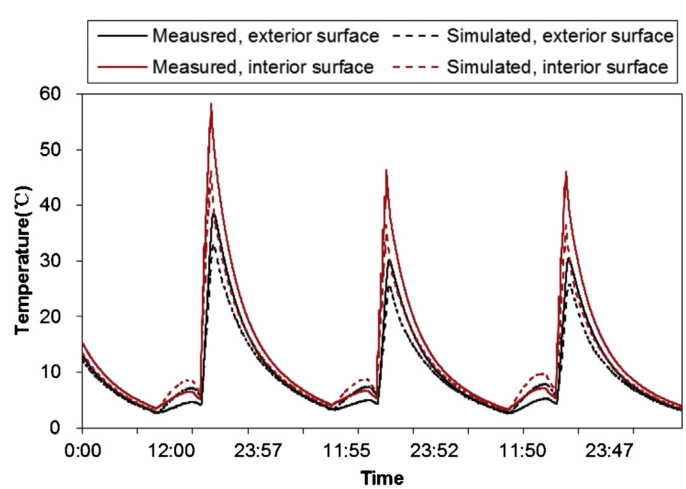

Fig. 4. Measured and calculated temperatures of the upper plate.

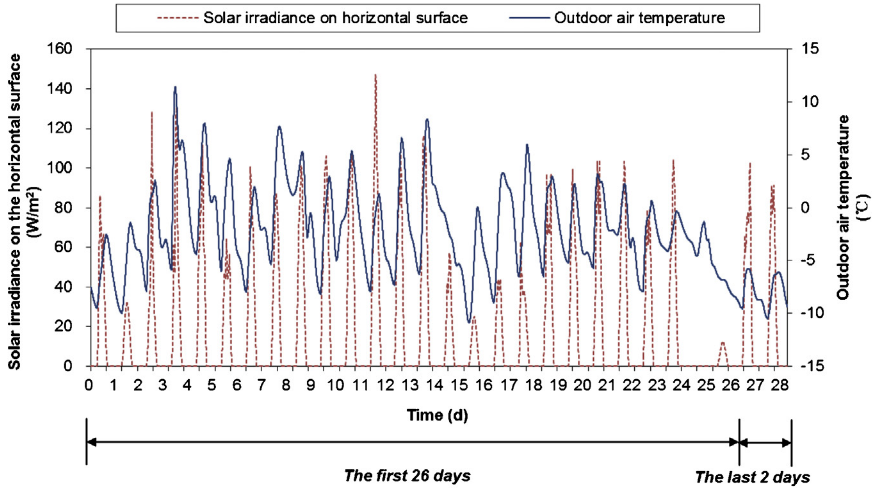

Fig. 5. The weather condition in the simulation.

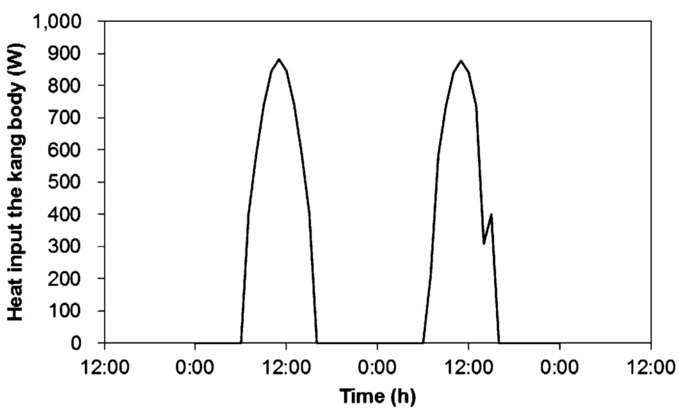

Fig. 6. The heat input to the kang air space during the simulation period.

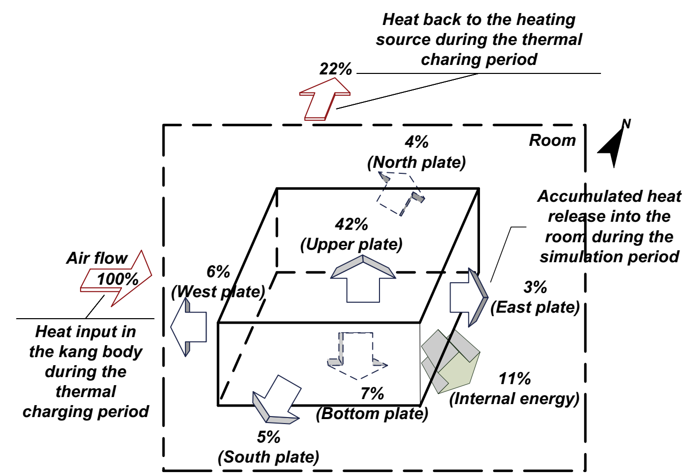

Fig. 8. Accumulative energy distribution of the kang body during the simulation period.

beneficial to boost the heat release into the room. In order to study this impact, we reduced the convective heat transfer resistance in the kang air space by increasing the interior surface area of the upper kang plate, which could be realized by making interior surface in V-groove shape. The quantity *Ratio*, defined as the interior surface area of the upper kang plate divided by the exterior surface area of the upper kang plate, is chosen to present the times of area increase from the base heat transfer area.

As Fig. 9 presents, there was no notable rise in the total energy storage of the kang body with the increase of the heat transfer area. This could be explained by the fact that the convection heat transfer coefficient in the kang air space varied around 5 W/(m^2 K) under such working scenario according to the heat transfer model [4], and

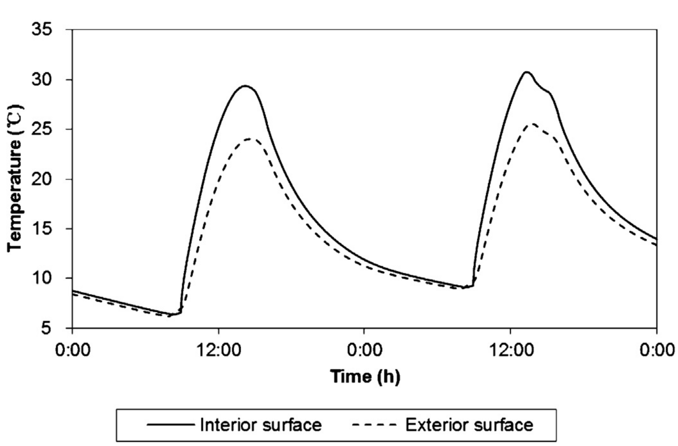

Fig. 7. Temperature variations of the upper kang plate.

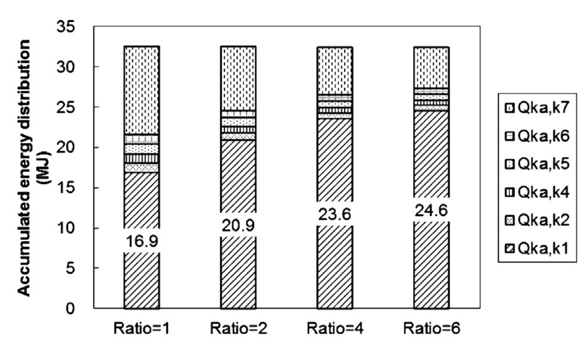

(Ratio=the interior surface area of the upper kang plate/the exterior surface area of the upper kang plate. In which, the interior surface area equals the convection heat transfer area between the airflow and the upper kang plate)

Fig. 9. The variations of the accumulated convection heat transfer between the airflow and the walls in the kang air space with the change of the interior surface area of the upper kang plate.

Table 2
Thermal capacity of the upper kang plate with variation of the thickness of the upper kang plate.

Thickness of the precast concrete	Specific heat (C_p)	Density (ρ)	Volume (V)	Thermal capacity ($C_\rho \rho V$)
	kJ/(kg K)	kg/m^3	m^3	kJ/K
50 mm			0.18	272.2
100 mm	0.84	1800	0.36	544.3
150 mm			0.54	816.5

the according heat transfer area reached around 8 m^2 when *Ratio* was only 1.0, so the convective heat transfer resistance in the pass could be as low as 0.03 K/W according to the definition. The value was so low that it would not decrease greatly with the increase of either the heat transfer area or the heat transfer coefficient due to the (−1) relationship of (*hF*).

Moreover, as the accumulated solar heat distribution shown in Fig. 9, with the increase of the heat transfer area, more convection heat was transferred to the upper kang plate, which was dominantly caused by the increase of the convective heat transfer area between the warm airflow and the upper kang plate, and thus the reduction of the convective heat transfer resistance accordingly. But it is noticed that such impact receded until the quantity *Ratio* turned to 4.0, namely the convective heat transfer would be increased by only 1.0 MJ when the quantity *Ratio* increased from 4.0 to 6.0. That was possibly caused by fact that the reduction of the convective heat transfer resistance between the upper kang plate and the warm airflow would not decrease greatly when the heat transfer area was big enough.

3.3. The impact of the thermal capacity of the upper kang plate

It is known that the upper kang plate with appropriate thermal capacity could maintain certain level of warmth during the required period, and therefore the thermal capacity of the upper kang plate is regarded as one of the critical parameters in the kang thermal design [10]. In order to study the impact of the thermal capacity on the thermal performance of the kang body, different thermal capacities were obtained by changing the thickness of the upper kang plate, as Table 2 presents, without affecting the thermal physical properties of the kang plate.

As Fig. 10 presents, the temperature varied at the lower level with larger thermal capacity during the solar heater working period, while at the upper level during the night. Under the simulation condition, the maximal interior surface temperature of the upper kang plate decreased from about 30 °C to 26 °C and that of the exterior surface dropped from around 25 °C to 18 °C when the thermal capacity of the upper kang plate increased from 272 kJ/K to 817 kJ/K, and the time delay of the kang plate increased to around 1.5 h accordingly. Therefore, the data pointed the temperature wave decay and time delay of the upper kang plate with the increase of the thermal capacity.

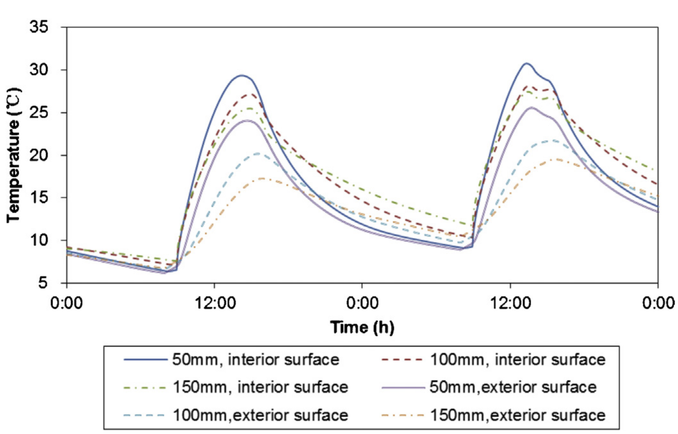

Fig. 10. Temperature variations of the upper kang plate with the increase of the thickness of the upper kang plate.

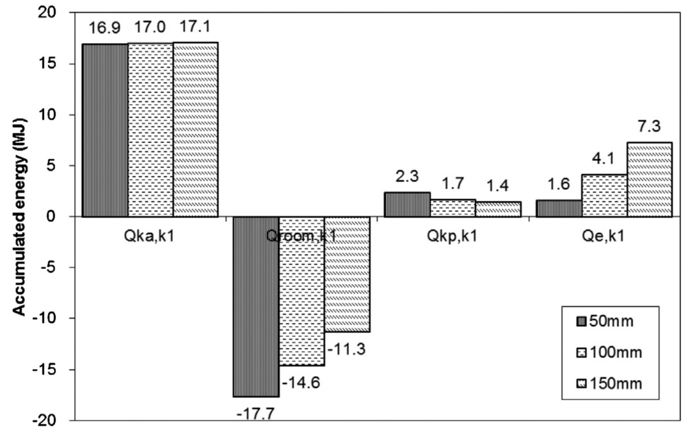

Fig. 11. Energy balance analyses of the upper kang plate with the increase of the thickness of the upper kang plate.

From the view of its thermal process presented in Fig. 11, the upper kang plate absorbed almost the same amount of convection heat from the warm airflow possibly due to the same convective heat transfer resistance in the pass. However, the average temperature of the kang plate decreased with the increase of the thermal capacity, and thus reduced the temperature differences between the room and the kang, also that between the interior surface of the upper kang plate and the other kang plates. That helped to decrease the heat release into the room, and the long-wave radiation to the other kang plates as well. On the basis of energy conservation, the reduction of this amount of heat was eventually transformed into internal energy of the kang plate during the simulation period.

3.4. The impact of the thermal conductivity of the upper kang plate

Increasing the thermal conductivity of the kang plate material could help to strengthen the thermal conduction along the thickness of the kang plate, leading to change of the thermal process in the kang body. In order to show the effect on the solar kang, we chose three thermal conductivity of the upper kang plate, 0.43 W/(m K), 0.93 W/(m K), and 2.93 W/(m K), whose value was close to that of solid brick, cement, and marble, respectively.

As Fig. 12 presents, the maximal temperature difference between the interior and exterior surface decreased from 9.4 °C to 2.3 °C with the thermal conductivity increased from 0.43 W/(m K) to 2.93 W/(m K), meaning that the increase of the thermal conductivity of the kang plate helped to decrease the temperature wave difference between the interior and exterior surface. That helped to enlarge the temperature differences between the interior surface of the upper kang plate and the warm airflow, as well as that between the interior surface of the upper kang plate and the partition plate, which led to more convective heat transfer from the warm airflow to the upper kang plate, and the long-wave radiation heat transfer from the partition plate to the upper kang plate as well. Finally, all the heat was eventually transformed into the heat released to the room on the basis of the energy conservation, as shown in Fig. 13.

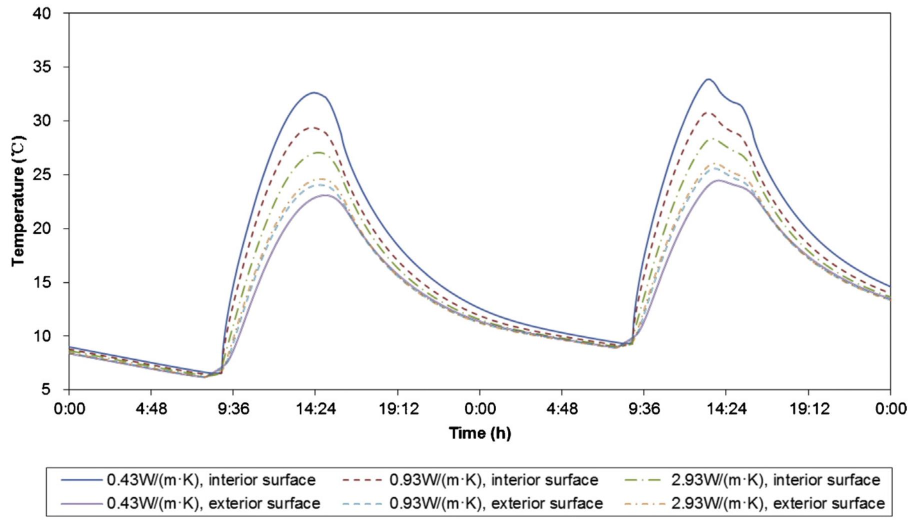

Fig. 12. Temperature variations of the upper kang plate with the change of the thermal conductivity (λ) of the upper kang plate.

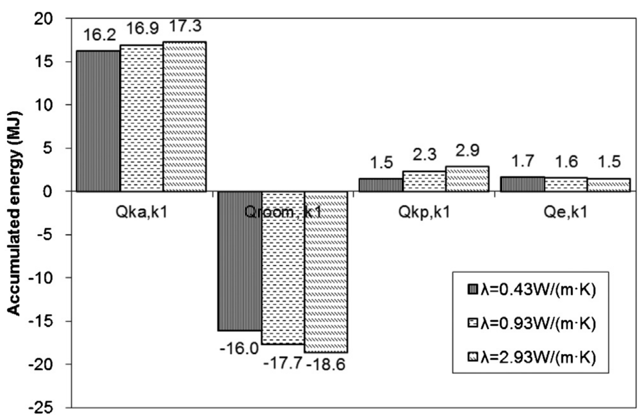

(Based on energy balance of the upper kang plate, $Q_{e,k1}=Q_{ka,k1}+Q_{kp,k1}+Q_{room,k1}$. In which, the heat transfer from the upper kang plate to the other component of the solar kang system is defined as the negative value, while the heat transfer is regarded as positive value in contrast.)

Fig. 13. Energy balance analyses of the upper kang plate with the changes of the thermal conductivity (λ) of the upper kang plate.

4. Conclusions

Using the numerical model developed previously for a new solar kang system, we conducted parametric analyses on kang's three parameters, namely the convective heat transfer resistance in the kang air space, the thermal capacity and the thermal conductivity of the upper kang plate, in the light of energy storage of the kang body, energy distribution, and the temperature variations of the upper kang plate. Simulation results have led to the following conclusions:

(1) Reducing the convective heat transfer resistance in the kang air space would not lead to notable rise of kang body's energy storage when only the solar collecting system worked, which was mainly due to large convective heat transfer area in the kang airflow pass. However, more convective heat could be transferred to the upper kang plate by increasing the convective heat transfer area between the upper kang plate and the warm airflow, but this effect would also diminish until the according convective heat transfer resistance became low enough.

(2) The thermal physical parameters of the upper kang plate, including the thermal capacity and the thermal conductivity, played a significant role in determining the thermal process in the kang body and its temperature variations. The upper kang plate with larger thermal capacity helped to decrease the heat release to the room and stored more solar heat during the simulation period. While, larger thermal conductivity of the upper kang plate would be beneficial to strengthen the convective heat transfer with the warm airflow and the long-wave radiation with the partition plate, and finally increased the heat release into the room.

Acknowledgement

The work is supported by the National Natural Science Foundation of China (NSFC), Project No. 51038005.

References

[1] X. Yang, Y. Jiang, M. Yang, et al., Energy and environment in Chinese rural housing: current status and future perspective, Frontiers of Energy and Power Engineering in China 4 (1) (2010) 35–46.
[2] Z. Zhuang, Y. Li, B. Chen, et al., Chinese kang as a domestic heating system in rural northern China – a review, Energy and Buildings 41 (2009) 111–119.
[3] H. Lin, M. Murray, T. Cohen, et al., Effect of smoking and solid-fuel use on COPD, lung cancer, and tuberculosis in China: a time-based, multiple risk factor, modelling study, Lancet 372 (2008) 1473–1483.
[4] M. Yang, X. Yang, P. Wang, et al., A new Chinese solar kang and its dynamic heat transfer model, Energy and Buildings 62 (2013) 539–549.
[5] D. Njomo, M. Daguenet, Sensitivity analysis of thermal performances of flat solar air heaters, Heat Mass Transfer 42 (2006) 1065–1081.
[6] J.A. Duffie, W.A. Bechman, Solar Engineering of Thermal Processes, John Wiley and Sons Inc., USA, 1991.
[7] X.L. Zhang, J.J. Xia, Z.Y. Jiang, et al., DeST – an integrated building simulation toolkit part I: fundamentals, Building Simulation 1 (2) (2008) 95–110.
[8] X.L. Zhang, J.J. Xia, Z.Y. Jiang, et al., DeST – an integrated building simulation toolkit part II: applications, Building Simulation 1 (3) (2008) 193–209.
[9] A. Bejan, Convection Heat Transfer, John Wiley and Sons Inc., USA, 1984.
[10] Z. Zhuang, Y. Li, B. Chen, Thermal storage performance analysis on Chinese kangs, Energy and Buildings 41 (2009) 452–459.